

Proceeding Paper

Catalytic Dye Degradation of Textile Dye Methylene Blue by Using Silver Nanoparticles Fabricated by Sustainable Approach [†]

Pradeep Kumar Pandey ^{1,*}, Joy Sarkar ^{1,*} and Shivangi Srivastava ²

¹ Department of Chemistry, Lucknow University, Lucknow 26007, India

² Department of Physics, Lucknow University, Lucknow-226007, India; shivangisrivastav007@gmail.com

* Correspondence: pradeepchemnano@gmail.com (P.K.P.); dr.joysarkar4@gmail.com (J.S.)

[†] Presented at the 2nd International Electronic Conference on Processes: Process Engineering—Current State and Future Trends (ECP 2023), 17–31 May 2023; Available online: <https://ecp2023.sciforum.net/>.

Abstract: A eco-friendly, cost effective, sustainable and green approach were used for the fabrication of silver nanoparticles by using leaf extract of *Blumea lacera* (Ag@BLE). Silver nanoparticles 9–13 nm sized were characterized by different analytical techniques. The analytical methodes utilized were powder X-ray diffraction (PXRD), Fourier-transformed infrared (FT-IR) and transmission electron microscopy (TEM). Intially synthesis of Ag@BLE nanoparticles were confirmed by UV-visible spectrophotometry and at 429 nm appeared a sharp surface plasmonic resonance (SPR) band. Organic dye methylene blue (MB) is one of the most abundant pollutants in the water environment. In the presence of catalyst Ag@BLE, the absorbance intensity of cationic MB dye was reduced dramatically by Sodium borohydride (NaBH₄). Methylene blue’s catalytic dye degradation was tested to determine the effectiveness and function of synthesized Ag@BLE, and the reduction rate were found to be 0.01455 min⁻¹ (0 mg Ag@BLE, 21 min), 0.03144 min⁻¹ (20 mg Ag@BLE, 24 min). Synthesized Ag@BLE showed rapid and excellent catalytic reduction of MB dye, and it follow pseudo first order kinetics.

Keywords: Silver nanoparticles; *Blumea lacera*; Dye degradation; Kinetics; Characterization

Citation: Pandey, P.K.; Sarkar, J.; Srivastava, S. Catalytic Dye Degradation of Textile Dye Methylene Blue by Using Silver Nanoparticles Fabricated by Sustainable Approach. *Eng. Proc.* **2023**, *37*, x. <https://doi.org/10.3390/xxxxx> Published: 17 May 2023



Copyright: © 2023 by the authors. Submitted for possible open access publication under the terms and conditions of the Creative Commons Attribution (CC BY) license (<https://creativecommons.org/licenses/by/4.0/>).

1. Introduction

Nanotechnology playing an important role to address several problems such as solar energy, waste water treatment, heavy metals sensing from waste water and nanomedicine, etc. [1]. Past few decades, researchers mainly focused on sustainable green approach for the synthesis of metal-based nanoparticles. Because of their huge surface area to volume ratio, practicality at lower temperatures, and unique physiochemical features such as thermal [2], optical [3] and electrical [4] properties, noble metal nanoparticles of gold and silver are gaining prominence in the field of nanomaterials research. For the plant based green synthesis of silver and gold nanoparticles their salts are required. For the large-scale synthesis preferentially used silver salt because it is less expensive than gold salt [5]. Since plants are the richest source of biomolecules such as lipids, polyphenol, proteins, carbohydrates, terpenoids, flavonoids and so on. These biomolecules are work as reducing and stabilizing agents [6,7]. A type of affordable, environmentally responsible, and biocompatible techniques known as “green synthesis” and it has numerous benefits over traditional procedures [8]. As a result, the current work uses *Blumea lacera* leaf extract to synthesis silver nanoparticles in an effort to develop a sustainable method and the synthesized Ag@BLE NPs used in the photocatalytic dye degradation of organic dyes methylene blue.

Water pollution is increased rapidly due to global industrialization and increasing organic dyes in the industrial waste water. It's very difficult to remove organic dyes from waste water due to low biodegradability and difficult to degraded [9]. Organic dyes are carcinogenic, highly toxicity and based on mainly aromatic azo or heterocyclic aromatic compounds. In the present time, it's very challenging task for the researcher to remove these harmful dyes from the waste water. During the last few decades, researchers are mainly focused to developed sustainable, easy to synthesized and cost effective nanomaterials [10]. Therefore, it is probable that nanomaterials will be developed to degraded dyes in aqueous solutions. At the moment, researchers are working on heterogeneous photocatalytic dye degradation of carcinogenic dyes from textile industries using semiconductor nanoparticles, since photocatalytic degradation of organic dyes is one of the most simple and cost-effective approaches for water treatment [9,11].

Therefore, the primary goal of this work is to develop a technique for the synthesis of Ag@BLE NPs utilizing *B. lacera* leaf extract. Various analytical techniques were used to characterize the synthesized Ag@BLE NPs, including UV-visible spectroscopy (UV-vis), FT-IR, field emission scanning electron microscopy (FE-SEM), TEM, and PXRD. Finally, the absorbance intensity of cationic MB by Sodium borohydride (NaBH_4) and the function and efficacy of AgNPs in the catalytic degradation of MB dye were investigated in the presence of a catalyst Ag@BLE. A comparative study table of catalytic dye degradation through AgNPs are given in Table 1.

Table 1. Comparison of biosynthesized AgNPs catalytic dye degradation.

| Synthesis of Nanoparticles (Source) | size | Targeted Dyes | Degradation Percentage (%) | References |
|-------------------------------------|--------------|---------------------------------|----------------------------|--------------------------|
| Sodium acetate | 8–40 nm | Methyl orange Methylene blue | 100 | [12] |
| Bacterial strain | 30–70 nm | Disperse blue 183 | 100 | [13] |
| K- carrageenan | 12 nm | Rhodamine B Methylene blue | 100 | [14] |
| Isoimperatorin | 79–200 nm | New Fuchsine | 96.5 | [15] |
| | | Methylene blue | 96 | |
| | | Erythrosine B | 92 | |
| Diaminobenzoic acid | 9.2 nm | Methyl orange | 99 < | [16] |
| | | Rhodamine B | | |
| | | Acridine | | |
| Ruellia tuberosa | 10–20 nm | Crystal violet | 87 | [17] |
| | | Coomassie | 74 | |
| Chlorella vulgaris | 55 nm | Methylene blue | 96 | [18] |
| Blumea lacera | 13 nm | Methylene blue | 56 | This present work |

2. Materials and Methods

The present experiment employed only analytical-grade chemicals and reagents. Both sodium hydroxide (NaOH , 99%) and silver nitrate (AgNO_3 , 99.90%) were utilized as received. Fabrication of AgNPs was carried out as described by [19,20]. To eliminate all dust particles, the leaf of the plant *B. lacera* was washed twice: once with tap water and once with double-distilled water. The leaves were utilised as starting biomass after being roughly sliced to 4–5 mm. Fresh materials (5 g) of biomass were boiled in a beaker with 50 mL of double-distilled water at 50 °C to reduce the volume by half. In order to employ the leaf extract in the fabrication of Ag@BLE NPs and used in the other experimental research, the mixture was filtered using Whatman filter paper no. 42 and the extract was stored at 5°C for future experiment. Ag@BLE NPs were fabricated by mixing 6 mL of *B. lacera* plant leaf extract and 14 mL of 1 mM silver nitrate at pH = 9.0, followed by 3 h of

constant stirring at 630 rounds per minute (rpm) at room temperature (RT). At the 429 nm SPR band, a colour change from light brown to dark brown suggested the fabrication of the Ag@BLE NPs. Additionally, high-speed centrifugation was used to further purify and produced Ag@BLE NPs. To remove contaminants from the Ag@BLE NPs residue, the produced Ag@BLE NPs were washed multiple times with double distilled water and then one more with 0.01% acetic acid. AgNPs were then lyophilized and reserved for future usage at 5 °C in an sealed ampule [19,21].

3. Results and Discussion

3.1. Morphological Studies

FE-SEM and TEM analysis were done for morphological and structural study. (Figure 1a) shows FE-SEM image of synthesized Ag@BLE NPs at a 1 μm and (Figure 1b) shows TEM image of NPs at a 20 nm. FE-SEM image of the sample has diversity in the surface morphology. The surface morphology of fabricated Ag@BLE NPs is quasi-spherical, with negligible agglomeration in the solid phase, as seen in FE-SEM image. TEM investigation was carried out to have a clear understanding of the shape and particle size of fabricated Ag@BLE NPs. The majority of the Ag@BLE NPs are shown to have semi-spherical or spherical shape, which is consistent with the FE-SEM findings. The average diameter of Ag@BLE NPs is near about 13.00 nm which is close to average crystalline size calculated from the XRD [9,19].

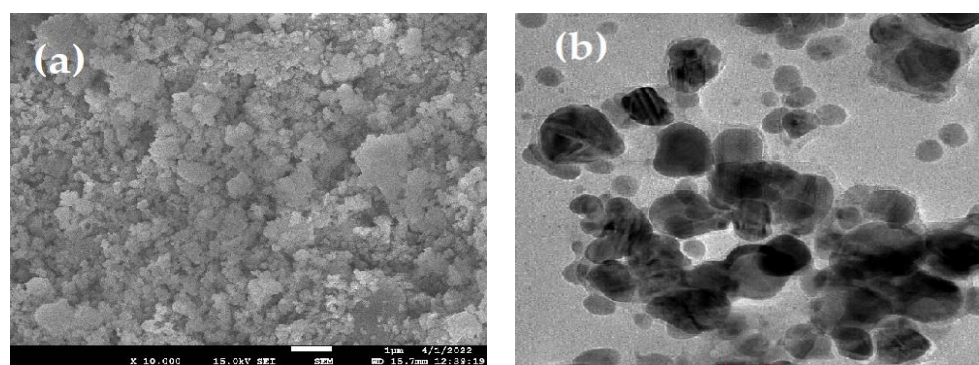


Figure 1. (a) FE-SEM image of AgNPs at a 1 μm and (b) TEM image of AgNPs at a 20 nm.

3.2. UV-Visible Analysis

The morphology and size of the NPs have a significant impact on their SPR band. So, for the initial verification of Ag@BLE NPs generation, UV-visible spectrophotometry became a crucial instrument. One peak at 325 nm can be found in the absorption spectrum of the *B. lacera* leaves extract (Figure 2). Ag@BLE NP formation revealed a shift in colour from pale brown to dark brown, which got darker with time. A prominent SPR band at 429 nm and a UV-visible spectrophotometer result corroborated this change in the solution's colour [5].

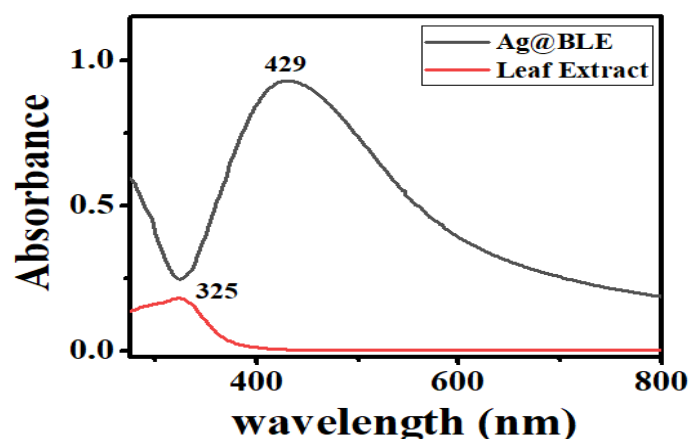


Figure 2. UV-visible spectra, peak at 325 nm for leaf extract *B. lacera* and peak at 429 nm for fabricated Ag@BLE NPs.

3.3. Powder X-ray Diffraction (PXRD) Analysis

PXRD data was acquired (Figure 3) to demonstrate the existence of crystalline silver in the fabricated Ag@BLE NPs by *B. lacera* leaf extract. Four peaks in the PXRD pattern of the synthesised Ag@BLE NPs stand out more than the others and are placed at 77.46° , 64.54° , 44.28° , and 38.16° , respectively. Their 2θ values are analogous to the (311), (220), (200), and (111), hkl planes, with the JCPDS file number 04-0783 showing the greatest similarity to each of these peaks [5,8]. PXRD indicates that the face-centered cubic structure (FCC) is what results from the reduction of silver ions and the resultant nanoparticles. The peak at 38.16° that corresponds to plane (111) is more intense than other peaks, indicating that the AgNPs are tiny and fine. The prominent peak reveals the presence of crystal-sized particles at the nanoscale [19].

Additionally, several peaks in the PXRD that are clearly visible (shown with a^*) at 57.50° , 54.84° , 46.26° , 32.28° , and 27.86° may be the result of metabolites capping the Ag@BLE NPs [5,19]. Using Debye-Scherrer's equation $D = 0.9\lambda/\cos\theta$, it was determined that the average crystalline size of Ag@BLE NPs was 10.960 nm. Here, D is the crystallite size, λ X-ray wavelength ($\lambda = 1.540 \text{ \AA}$), β full width at half maximum (FWHM) of the relevant peak, and diffraction angle (θ) are all given.

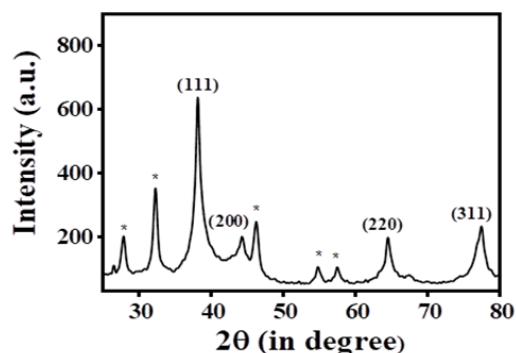


Figure 3. Pattern of powder X-ray diffraction (PXRD) for Ag@BLE NPs.

3.4. Fourier Transformed Infrared Analysis

The Fourier Transformed Infrared (FT-IR) spectra of synthesised Ag@BLE NPs ranged from 3680 to 380 cm^{-1} (Figure 4). FT-IR study shows that phytochemicals such as alkaloids, polyphenols, amino acids flavonoids, triterpenoids, proteins and so on acted as both a capping and stabilising agent. The FT-IR band at 3484 cm^{-1} is caused by $-\text{NH}$, $-\text{OH}$ stretching vibration. Two weak bands were detected at 2912 and 2328 cm^{-1} , matching to

the C-H stretching frequency of the aliphatic methylene group and the overtone of the aromatic fragment's C-H bending, respectively. Carbonyl compounds' C=O stretching vibration produces a band at 1821 and 1637 cm^{-1} . Because of the stretching of the aromatic fragment's sp^2 hybridised carbon-carbon double bond, a band at 1536 cm^{-1} was seen. A band corresponding to the -C-O group was found at 1388 cm^{-1} . Due to the C-H group of rings bending in plane or stretching, a band at 1083 cm^{-1} was seen. Due to the inter-atomic absorption vibration of silver metal, three bands may be seen in the lower area below 900 cm^{-1} [8,19]. Therefore, it can be inferred from the FT-IR study that the various functional groups connected to the phytochemicals stabilise Ag@BLE NPs in colloidal form when they are present in an aqueous solution. Therefore, these functional groups operate as stabilising and reducing agents.

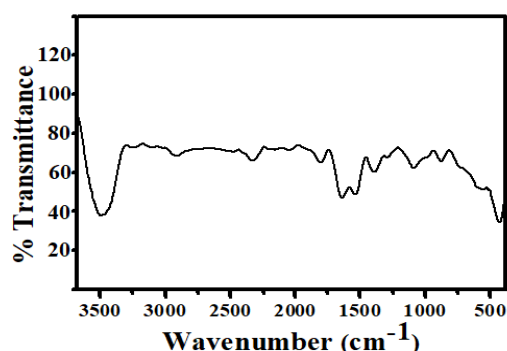


Figure 4. FT-IR spectrum of synthesized Ag@BLE NPs.

4. Catalytic Performance of Ag@BLE NPs in the Degradation of Textile Dye Methylene Blue (MB)

The benefits of photocatalytic degradation over other approaches, a photocatalytic reaction is a chemical process that occurs under the combined action of light and the photocatalyst. This method has various advantages, including environmental protection, total pollution degradation, and no secondary contamination. Here, NaBH_4 work as a reducing agent and taking into consideration as a reference, the degradation of the textile dye MB was studied using the crystalline Ag@BLE NPs. The absorption spectra of MB (80 M) in double-distilled water with NaBH_4 without and with Ag@BLE nanoparticles are shown in (Figure 5). Around 664 nm in the UV-visible spectrum, MB became visible due to lower energy absorption band $n-\pi^*$ transitions [11]. Due to the reduction and stabilization of MB in the presence of NaBH_4 , the absorbance intensity somewhat lowers (Figure 5a). The absorbance intensity falls monotonically with the addition of 20 mg Ag@BLE NPs (Figure 5b). This shows that MB degrades to Leuco MB in the presence of Ag@BLE NPs. As a result, Ag@BLE NPs serve as an active catalyst while NaBH_4 works as a reducing agent.

$R = [(C_0 - C_t)/C_0] \times 100$ is a formula used to evaluate the ability of Ag@BLE NPs to degrade MB. C_0 and C_t stand for the absorbance of MB at time $t = 0$ and time t , respectively. Whereas the reaction rate constant for the degradation of MB is calculated using the formula $\ln(C_t/C_0) = -kt$, where k is the reaction rate constant and t represents the passage of time. (Figure 5c) provides linear relations and a plot of $\ln(C_t/C_0)$ vs. t . The linear graphs showed that the rate of MB degradation is pseudo-first order kinetics. [10]. In the absence of Ag@BLE NPs, the value of rate constant (k) is 0.01455 min^{-1} (0 mg Ag@BLE, 21 min) and in the presence of 20 mg Ag@BLE NPs the value of k is 0.03144 min^{-1} (20 mg Ag@BLE, 24 min).

The presence of Ag@BLE NPs stimulates the decomposition of MB. By aiding the electron from BH_4^- species (acting as the donor) to the excited MB (acting as the acceptor) via Ag@BLE NPs, which were acquiring and transfusing electrons from the donor to the acceptor, Ag@BLE NPs catalyse the reduction of MB in the degradation of dye [9,11].

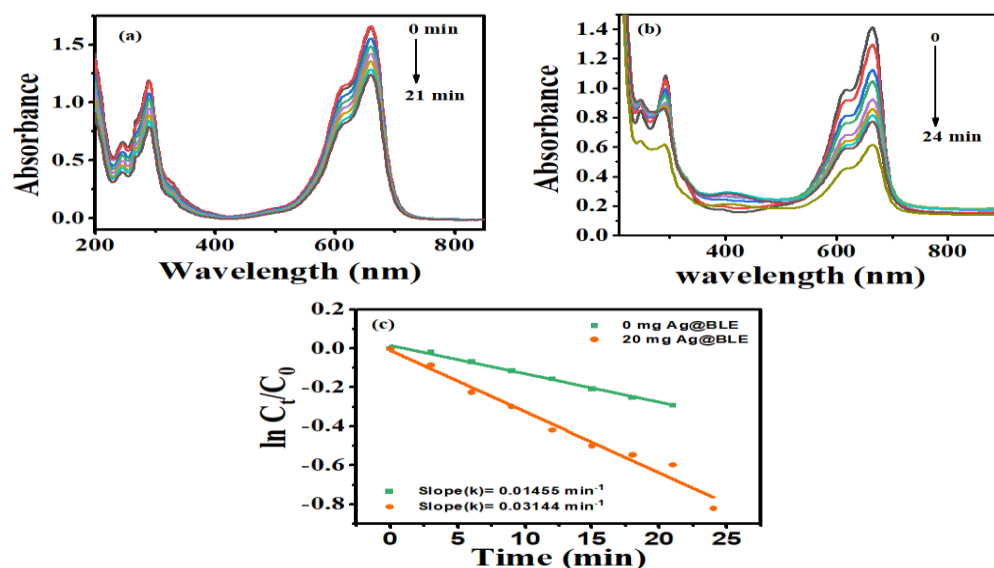


Figure 5. Methylene blue (MB) dye absorption spectra over time in the presence of NaBH_4 as a reducing agent (a) without catalysis and (b) catalyzed with 20 mg Ag@BLE NPs, as well as digital images (insets of (a,b)) showing before and after the reaction (c) The plot of the MB's $\ln(C_t/C_0)$ as a function of time (t) in the presence of 0.0 mg and 20 mg AgNPs and first-order reaction rate constants k (in min^{-1}).

5. Conclusions

The plant *B. lacera* is used to effectively fabricate nano-sized Ag@BLE NPs in the current paper, which is then successfully characterized using a variety of analytical methods. PXRD confirms the presence of Ag@BLE NPs and found the crystallite size of 10.960 nm, FTIR confirms the different functional groups, UV-visible confirms the *B. lacera* leaf extract at 325 nm and Ag@BLE NPs formation at the 429 nm absorbance, lastly FESEM shows the non-spherical and quasi-spherical morphology and TEM confirms the average diameter of the AgNPs were 13 nm. Furthermore, Ag@BLE NPs is successfully applicable for MB catalytic degradation and rate of degradation increases in the presence of Ag@BLE NPs.

Author Contributions: All authors are equally contributed to data analysis, drafting or revising the article, gave final approval of the version to be published, and agree to be accountable for all aspects of the work. All authors have read and agreed to the published version of the manuscript.

Funding: This study received no particular support from governmental, commercial, or not-for-profit funding entities.

Acknowledgments: The authors are highly grateful to the Head of Department (HoD), Department of Chemistry (DoC), University of Lucknow (UoL), Lucknow (U.P.) India, for providing basic infrastructure facilities, like UV-visible spectrophotometry, and FT-IR spectroscopy for performing experimental work. The authors are also grateful to the Head of Department (HoD), Department of Physics (DoP), University of Lucknow (UoL), Lucknow (U.P.) India, All India Institute of Medical Science (AIIMS), New Delhi, and Birbal Sahni institute of Palaeosciences, Lucknow, U.P. India, for providing X-ray diffraction, transmission electron microscopy and field emission scanning electron microscopy facilities respectively.

Conflicts of Interest: There are no conflicts of interest, according to the authors.

References

1. Seku, K.; Hussaini, S.S.; Pejjai, B.; Al Balushi, M.M.S.; Dasari, R.; Golla, N.; Reddy, G.B. A rapid microwave-assisted synthesis of silver nanoparticles using *Ziziphus jujuba* Mill fruit extract and their catalytic and antimicrobial properties. *Chem. Pap.* **2020**, *75*, 1341–1354. <https://doi.org/10.1007/s11696-020-01386-w>
2. Vykoukal, V.; Zelenka, F.; Bursik, J.; Kana, T.; Kroupa, A.; Pinkas, J. Thermal properties of Ag@Ni core-shell nanoparticles. *Calphad* **2020**, *69*, 101741. <https://doi.org/10.1016/j.calphad.2020.101741>
3. Wiley, B.J.; Chen, Y.; McLellan, J.M.; Xiong, Y.; Li, Z.-Y.; Ginger, D.; Xia, Y. Synthesis and Optical Properties of Silver Nanobars and Nanorice. *Nano Lett.* **2007**, *7*, 1032–1036. <https://doi.org/10.1021/nl070214f>
4. Saini, I.; Rozra, J.; Chandak, N.; Aggarwal, S.; Sharma, P.; Sharma, A. Tailoring of electrical, optical and structural properties of PVA by addition of Ag nanoparticles. *Mater. Chem. Phys.* **2013**, *139*, 802–810. <http://dx.doi.org/10.1016/j.matchemphys.2013.02.035>
5. Gangwar, C.; Yaseen, B.; Kumar, I.; Singh, N.K.; Naik, R.M. Growth Kinetic Study of Tannic Acid Mediated Monodispersed Silver Nanoparticles Synthesized by Chemical Reduction Method and Its Characterization. *ACS Omega* **2021**, *6*, 22344–22356. <https://doi.org/10.1021/acsomega.1c03100>
6. AlNadhari, S.; Al-Enazi, N.M.; Alshehrei, F.; Ameen, F. A review on biogenic synthesis of metal nanoparticles using marine algae and its applications. *Environ. Res.* **2020**, *194*, 110672. <https://doi.org/10.1016/j.envres.2020.110672>
7. Anandalakshmi, K.; Venugobal, J.; Ramasamy, V. Characterization of silver nanoparticles by green synthesis method using *Pedalium murex* leaf extract and their antibacterial activity. *Appl. Nanosci.* **2015**, *6*, 399–408. <https://doi.org/10.1007/s13204-015-0449-z>
8. Gangwar, C.; Yaseen, B.; Kumar, I.; Nayak, R.; Sarkar, J.; Baker, A.; Kumar, A.; Ojha, H.; Singh, N.K.; Naik, R.M. Nano palladium/palladium oxide formulation using *Ricinus communis* plant leaves for antioxidant and cytotoxic activities. *Inorg. Chem. Commun.* **2023**, *149*, 110417. <https://doi.org/10.1016/j.inoche.2023.110417>
9. Kumar, I.; Gangwar, C.; Yaseen, B.; Pandey, P.K.; Mishra, S.K.; Naik, R.M. Kinetic and Mechanistic Studies of the Formation of Silver Nanoparticles by Nicotinamide as a Reducing Agent. *ACS Omega* **2022**, *7*, 13778–13788. <https://doi.org/10.1021/acsomega.2c00046>
10. Chandra, R.; Nath, M. Controlled synthesis of AgNPs@ZIF-8 composite: Efficient heterogeneous photocatalyst for degradation of methylene blue and congo red. *J. Water Process. Eng.* **2020**, *36*, 101266. <http://dx.doi.org/10.1016/j.jwpe.2020.101266>
11. Mehata, M.S. Green route synthesis of silver nanoparticles using plants/ginger extracts with enhanced surface plasmon resonance and degradation of textile dye. *Mater. Sci. Eng. B* **2021**, *273*, 115418. <https://doi.org/10.1016/j.mseb.2021.115418>
12. Gola, D.; Kriti, A.; Bhatt, N.; Bajpai, M.; Singh, A.; Arya, A.; Chauhan, N.; Srivastava, S.K.; Tyagi, P.K.; Agrawal, Y. Silver nanoparticles for enhanced dye degradation. *Curr. Res. Green Sustain. Chem.* **2021**, *4*, 100132. <https://doi.org/10.1016/j.crgsc.2021.100132>
13. Nazari, N.; Kashi, F.J. A novel microbial synthesis of silver nanoparticles: Its bioactivity, Ag/Ca-Alg beads as an effective catalyst for decolorization Disperse Blue 183 from textile industry effluent. *Sep. Purif. Technol.* **2020**, *259*, 118117. <https://doi.org/10.1016/j.seppur.2020.118117>
14. Pandey, S.; Do, J.Y.; Kim, J.; Kang, M. Fast and highly efficient catalytic degradation of dyes using κ -carrageenan stabilized silver nanoparticles nanocatalyst. *Carbohydr. Polym.* **2019**, *230*, 115597. <https://doi.org/10.1016/j.carbpol.2019.115597>
15. Mavaei, M.; Chahardoli, A.; Shokoohinia, Y.; Khoshroo, A.; Fattahi, A. One-step Synthesized Silver Nanoparticles Using Isoimperatorin: Evaluation of Photocatalytic, and Electrochemical Activities. *Sci. Rep.* **2020**, *10*, 1–12. <https://doi.org/10.1038/s41598-020-58697-x>
16. Chandhru, M.; Rani, S.K.; Vasimalai, N. Reductive degradation of toxic six dyes in industrial wastewater using diaminobenzoic acid capped silver nanoparticles. *J. Environ. Chem. Eng.* **2020**, *8*, 104225. <https://doi.org/10.1016/j.jece.2020.104225>
17. Seerangaraj, V.; Sathiyavimal, S.; Shankar, S.N.; Nandagopal, J.G.T.; Balashanmugam, P.; Al-Misned, F.A.; Shanmugavel, M.; Senthilkumar, P.; Pugazhendhi, A. Cytotoxic effects of silver nanoparticles on *Ruellia tuberosa*: Photocatalytic degradation properties against crystal violet and coomassie brilliant blue. *J. Environ. Chem. Eng.* **2021**, *9*, 105088. <https://doi.org/10.1016/j.jece.2021.105088>
18. Rajkumar R.; Ezhumalai, G.; Gnanadesigan, M. A green approach for the synthesis of silver nanoparticles by *Chlorella vulgaris* and its application in photocatalytic dye degradation activity. *Environ. Technol. Innov.* **2020**, *21*, 101282. <https://doi.org/10.1016/j.eti.2020.101282>
19. Pandey, P.K.; Gangwar, C.; Yaseen, B.; Kumar, I.; Nayak, R.; Kumar, S.; Naik, R.M.; Banerjee, M.; Sarkar, J. Anticancerous and antioxidant properties of fabricated silver nanoparticles involving bio-organic framework using medicinal plant *Blumea lacera*. *Chem. Pap.* **2023**, 1–15. <https://doi.org/10.1007/s11696-023-02723-5>

20. Jadhav, K.; Deore, S.; Dhamecha, D.; R, R.H.; Jagwani, S.; Jalalpure, S.; Bohara, R. Phytosynthesis of Silver Nanoparticles: Characterization, Biocompatibility Studies, and Anticancer Activity. *ACS Biomater. Sci. Eng.* **2018**, *4*, 892–899. <https://doi.org/10.1021/acsbomaterials.7b00707>
21. Garibo, D.; Borbón-Nuñez, H.A.; de León, J.N.D.; Mendoza, E.G.; Estrada, I.; Toledano-Magaña, Y.; Tiznado, H.; Ovalle-Marroquin, M.; Soto-Ramos, A.G.; Blanco, A.; et al. Green synthesis of silver nanoparticles using *Lysiloma acapulcensis* exhibit high-antimicrobial activity. *Sci. Rep.* **2020**, *10*, 12805. <https://doi.org/10.1038/s41598-020-69606-7>

Disclaimer/Publisher's Note: The statements, opinions and data contained in all publications are solely those of the individual author(s) and contributor(s) and not of MDPI and/or the editor(s). MDPI and/or the editor(s) disclaim responsibility for any injury to people or property resulting from any ideas, methods, instructions or products referred to in the content.